

On-site analysis of archaeological artifacts excavated from the site on the outcrop at Northwest Saqqara, Egypt, by using a newly developed portable fluorescence spectrometer and diffractometer

Yoshinari Abe · Izumi Nakai · Kazumitsu Takahashi ·
Nozomu Kawai · Sakuji Yoshimura

Received: 3 June 2009 / Revised: 7 September 2009 / Accepted: 8 September 2009 / Published online: 1 October 2009
© Springer-Verlag 2009

Abstract Blue-painted pottery was produced in the New Kingdom, Egypt, and decorated with blue, red, and black pigment. In this study, two newly developed portable instruments, a portable X-ray fluorescence spectrometer and a portable X-ray powder diffractometer, were brought to the site on the outcrop at Northwest Saqqara, an archaeological site in Egypt, to verify their performance in on-site analysis of excavated artifacts at the site. Pigments used for the blue-painted pottery and plasters in the New Kingdom were analyzed by these instruments on the basis of both their chemical compositions and crystal-structural information. The blue pigments were identified as two different pigments, Egyptian blue and cobalt blue. The diffraction pattern of the blue pigment of the painted pottery exhibited that of spinel structure. The XRF spectrum of the blue pigment obtained by the same instrument from the same position indicates the presence of Mn, Co, Fe, Ni, and Zn. The possibility of compositional transitions of the cobalt blue pigment with time was revealed on by detailed analysis of the XRF data. The reason for the transitions is considered together with the archaeological background of the New Kingdom, Egypt.

Keywords Archaeometry · Portable XRF · Portable XRD · Cobalt blue · On-site analysis

Introduction

As scientific analytical techniques are increasingly used for archaeological study, a new discipline, “Archaeochemistry”, has been established. Recently, synchrotron radiation X-ray analyses have been widely used for archaeological study. This technique enables us to gather several types of information from the archaeological artifact [1–3]. In today’s Egypt, however, national laws exert tight control over the care of archaeological artifacts and their export from Egypt. These laws prohibit the taking of artifacts abroad for analysis. As a result, the variety and number of archaeological samples available for scientific analyses are limited. To overcome this obstacle, researchers in recent years have begun to carry out on-site analysis of archaeological artifacts by utilizing portable instruments [4–8]. We have therefore been continuously developing new portable instruments, a portable X-ray fluorescence spectrometer (XRF) [9–14] and an X-ray diffractometer (XRD) [9, 10, 15–17], designed for archaeological artifacts, and these instruments have been used at various archaeological sites and museums. Although portable XRF has become popular, portable XRD is rare. Uda et al. developed a portable XRD with an XRF function similar to our instrument, although their instrument uses Cr tube and the total weight is much heavier than our instrument (more than 30 kg) [7, 8]. Recently, another diffractometer with an energy-dispersive CCD as a detector has been developed by Chiari et al. [18]. Because an archaeological artifact often consists of several crystalline phases, combined analysis by XRF and XRD

Y. Abe · I. Nakai (✉)
Department of Applied Chemistry, Tokyo University of Science,
1-3, Kagurazaka, Shinjuku-ku,
Tokyo 162-8601, Japan
e-mail: inakai@rs.kagu.tus.ac.jp

K. Takahashi · N. Kawai · S. Yoshimura
Institute of Egyptology, Waseda University,
120-3-103, 513, Waseda-tsurumaki-cho Shinjuku-ku,
Tokyo 169-8050, Japan

allows accurate phase identifications of the artifact. Furthermore, when discussion of the detailed composition of a certain phase is necessary, combined use of XRF and XRD techniques helps the matter a great deal. In fact, these instruments were applied to detailed analysis of the blue pigments used in ancient Egypt in this study.

The two portable instruments were brought to the site on the outcrop at Northwest Saqqara, an archaeological site in Egypt, and were used for on-site analysis of excavated artifacts. This site is located approximately 2 km to the northwest of the famous Step Pyramid of Djoser at Saqqara, Egypt (refer to the map of Egypt in Fig. 1) and has been excavated by a team from the Institute of Egyptology, Waseda University, since 1991 [19, 20] (General director S. Yoshimura). The team unearthed a monument of Prince Khaemwaset, the fourth son of Ramesses II of the 19th Dynasty, and a mud-brick structure associated with Amenhotep II and Thutmose IV of the middle 18th Dynasty. It is expected that these remains will provide us with important archaeological evidence regarding the region of the Memphite area in the New Kingdom.

In this work we studied the pigments used in the “blue-painted pottery” and plaster painting excavated from the site. It is reported that blue-painted pottery from Northeast Saqqara can be typologically classified into three groups [20] belonging to the middle 18th Dynasty, the later 18th Dynasty, and the 19th Dynasty. The middle 18th Dynasty can also be divided into two sub-groups, the early half and the late half of this period. The pottery shards were decorated with pigments of three colors: blue, red, and black, which will be identified by a combined use of portable XRF and XRD in this study. We then focused on the compositional transition of the blue pigment of the blue-

painted pottery in relation to the typological transition of the pottery described below. The features of each pottery groups are summarized in the following section. Photographs of typical shards of each group are shown in Fig. 2.

The middle 18th Dynasty belongs to the reigns of Amenhotep II (1427–1401 BC) and Thutmose IV (1401–1391 BC). The pottery of this period is predominately made of “Marl clay”, which is fired to uniform pale yellow and rich in Ca. The most important characteristic of the pottery of this period is the presence of an ochreous substrate under the decoration. There are, in addition, two kinds of substrates, ochreous clay or a coating with ochreous slip on the surface. Ochreous clay (called Marl clay) is rich in Ca. In contrast, Fe-rich clay (called Nile silt) was used when there was an ochreous slip coating. The slip serves as a whitish background for the decoration, with the firing process making the Nile silt a reddish color. The decorations on the blue-painted pottery during this period show some changes over time; in the early half of this period, mainly faunal and floral motifs, such as birds, cows and lotus flowers, tend to be drawn realistically (Fig. 2). These paintings are also decorated with colorful lines and generally give us a colorful impression. As time passed, however, in the late half of this period, the decorations lost their realism and became more abstract. There was a growing tendency to use motifs with a geometrical design for animals and plants (Fig. 2). While many shards of blue-painted pottery have been excavated at these remains, the highest proportion of finds belongs to this period. The later 18th Dynasty corresponds to the period of the reigns of Amenhotep IV (Akhenaten) and Thatunkhamun (1353–1336 BC). In this period, the fabric used in the blue-painted pottery from North Saqqara was restricted to Nile silt. While ochreous slip could still be found, as in the middle 18th Dynasty, most of the painting lay directly on reddish clay. The design of the decorations had also changed, being based predominantly on repeating motifs of the lotus petals tapering downwards with a black outline and blue filling. Red pigment was only used for partial accentuation. In addition, the thickness of the blue paintings seems thinner than in the middle 18th Dynasty, although it remains unclear whether this thinness was caused by the technology used or the materials. Compared with other periods, there have been fewer excavated shards belonging to this period. The 19th Dynasty group from the site corresponds primarily to the reign of Ramesses II (1279–1213 BC), based on the discovery of a monument belonging to his fourth son, Prince Khaemwaset. The pottery of this period was made of Nile silt, the same as that of the last period, and cream slip coating was also used. The designs of the decorations became less complex, and there was growing tendency to use a large filling of blue pigment without elaboration. While there is the same tendency toward the blue painting being somewhat thin, as in the previous period, the blue areas are relatively homogeneous

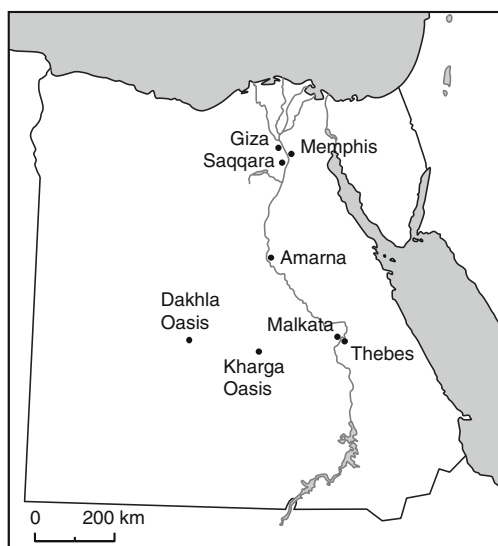


Fig. 1 Map of ancient Egypt



Fig. 2 Typological transition of blue-painted pottery excavated from Northwest Saqqara

and unspotted (Fig. 2). Black and red pigments were limited to use as fine lines, so that most of the surfaces were covered by blue filling.

Previous research on these artifacts has focused primarily on the finds from the palatial site of Malkata and Amarna belonging to the reign of Amenhotep III and that of Akhenaten respectively, the later 18th Dynasty, the peak of production of the blue-painted pottery [21–25]. Much remains unknown, however, regarding pottery dating to the middle 18th Dynasty, which corresponds to the early phase of its production, because few finds belonging to this period were excavated at these sites. The shards of pottery dating to the middle 18th Dynasty from the current site will give us new evidence about the early production of the pottery. The blue painted pottery from this site also would allow us to trace historical development of the blue painted pottery in the New Kingdom since shards dating to the later 18th Dynasty and 19th Dynasty are also found from the site. In addition, various colors of plaster pigments were also found at the site being likely to be fragments of the wall paintings of the mud-brick structure. The purpose of the work discussed in this paper was, therefore, to carry out accurate phase identification and chemical characterization of the various pigments in the New Kingdom, Egypt, based on both the chemical composition and the crystal structure by utilizing portable instruments developed by us, and to verify the performances of the instruments in on-site analysis.

Experimental

We brought two portable instruments to the site and used them for on-site analysis of the finds. The following includes details regarding these instruments and the samples analyzed.

Portable X-ray fluorescence spectrometer

The portable X-ray fluorescence spectrometer, the Oursstex 100FA-II (Fig. 3), was jointly developed by Oursstex Corporation [9–14] and our laboratory. This instrument is composed of a high-voltage power supply, a counting circuit controller, a spectrometer, a small vacuum pump, a

lap-top computer, and an external water-cooling system. This instrument can easily be brought to nearly anywhere both domestically and overseas because its total weight is only approximately 25 kg. The open-designed measurement head (spectrometer) allows it to be used for any shape and size of sample. This instrument uses an X-ray tube with a Pd target, and two modes of excitation are available: i.e. a monochromatic X-ray mode utilizing a pyrolytic (0002) crystal to obtain Pd-K line X-rays for the analysis of medium to heavy elements, and a white X-ray mode for analysis of both light elements and heavier elements. Using both X-ray modes and 40-kV X-ray tube, highly sensitive analysis of elements with atomic number greater than that of Na can be carried out. The SDD (silicon drift detector) was adapted as a detector and cooled to the operating temperature by an internal Peltier device and an external water-cooling system. This combined cooling system enables stable behavior in an environment as severe as the Egyptian summer that was encountered in this study. With these features, this instrument has the world's highest level of sensitivity among such portable instruments. The measurement conditions used for the X-ray fluorescence spectrometry are shown in Table 1.

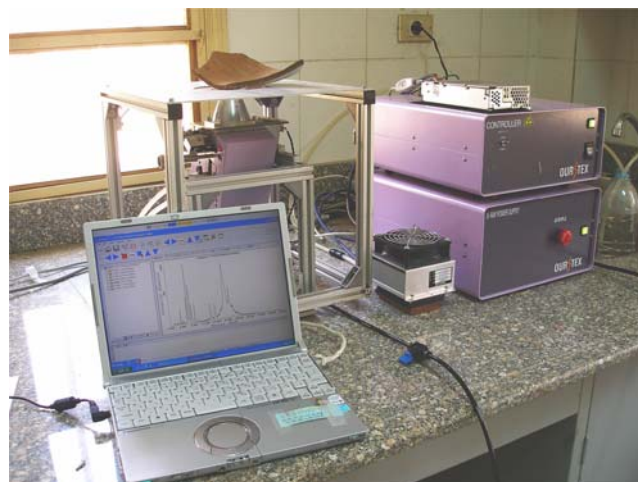


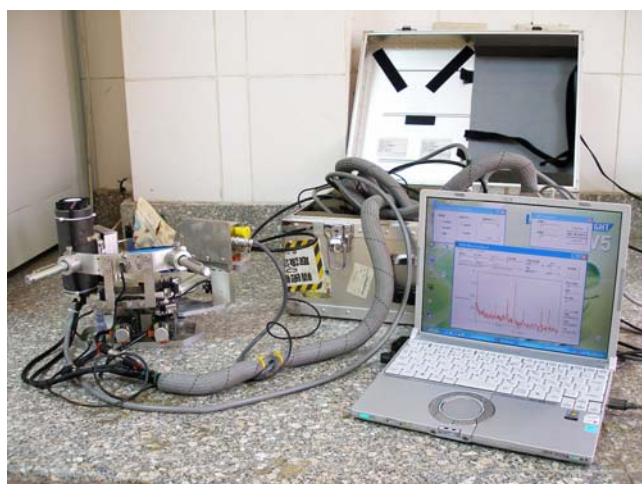
Fig. 3 A view of on-site analysis of painted pottery using the Oursstex 100FA-II portable X-ray fluorescence spectrometer

Table 1 Measurement conditions for X-ray fluorescence spectrometry and X-ray powder diffractometry

	Portable X-ray fluorescence spectrometer, Ourstex 100FA-II	Portable X-ray powder diffractometer, X-tec PT-APXRD
Manufacturer	Ourstex Co.	X-tec Co.
X-ray tube	Pd target	Cu target
Detector	SDD	Si-PIN
Cooling	Peltier system+Water cooling	Air
Tube voltage	40 kV	30 kV
Tube current	White X-ray mode: 0.25 mA; Mono. X-ray mode: 1.00 mA	0.3 mA
Measurement time	300 s (Real time)	3 or 6 s/step(0.1°)

Portable X-ray powder diffractometer

We have developed a portable X-ray powder diffractometer, X-tec PT-APXRD (Fig. 4) in cooperation with X-tec (Institute of X-Ray Technologies) [9, 10, 15–17]. The instrument is composed of a goniometer unit, a measurement-controller unit, and a lap-top computer. This instrument can be stored in a portable trunk case, and the total weight is 15 kg, giving it good portability. We have adopted Cu as the target of the X-ray tube (Oxford Instruments) and Si-PIN as a detector (Amptek XR100CR), which enables us to obtain a good powder diffraction pattern with low background. X-rays from the tube are focused by the slit and collimator and are used to irradiate the sample. Both the X-ray tube and the detector roll along the arc-shaped rail on the basal plate, around the θ -rotation axis of

**Fig. 4** A view of on-site analysis of painted pottery using the X-tec PT-APXRD portable X-ray powder diffractometer

the goniometer. The sample is placed on the θ -rotation axis using two laser pointers and an ultrasonic sensor, which are useful for nondestructive analysis of artifacts. The standard measurement conditions for X-ray powder diffractometry are also shown in Table 1. The zero point is adjusted by measurement of a direct beam using an adjusting jig. Silicon powder (NIST-SRM640c) was measured as a standard sample so that the accuracy of the measurement could be estimated. Additionally, this instrument was improved to adopt the function of the X-ray fluorescence spectrometer. With this modification, the instrument allowed us to carry out more reliable identification of unknown materials based on both the chemical composition and the crystal structure. However, in this study, we used X-ray fluorescence spectra obtained by use of the Ourstex 100FA-II because of the requirement for high resolution XRF spectra, as described below.

Samples

For precise phase identification of each pigment and the slip surface of the blue-painted pottery, the shards excavated at this site were nondestructively measured by both X-ray fluorescence spectrometry (XRF) and X-ray powder diffractometry (XRD). Using compositional information obtained with the XRF, we additionally examined a chronological transition of blue pigment. As previously noted, the shard surfaces were often covered with deposited salts, e.g., rock salt or gypsum. Taking into account the resulting salt deposition, a measurement point was selected on the basis of an observation with an optical microscope. The number of measured points per sample depended on the surface condition. Up to four points in a sample were measured in the case of bad condition, whereas only one point was measured for well-preserved sample. A total of 67 shards of blue-painted pottery were selected for analysis; 40 shards from the middle 18th Dynasty, nine shards from the later 18th Dynasty, and 18 shards from the 19th Dynasty [20]. We also measured plaster pigments (blue, red, and black) and analyzed a bright blue pigment remaining inside the pottery, indicating that the pottery was used as a container for blue pigment. We compared these pigments with that of the blue-painted pottery. All of these finds date to the New Kingdom. These painted plasters were fragments from the paintings on the wall of a mud-brick structure dating to the 18th Dynasty [20]. The analyses were performed at the storage magazine.

Peak fitting of the X-ray fluorescence spectrum

In XRF analysis of cobalt blue, peak overlapping becomes a serious problem because of the coexistence of Mn, Fe, Co, Ni, and Zn. We thus adopted peak separation based on

theoretical calculations to determine the accurate, integrated peak intensity of each element using WinQXAS software for analysis of the X-ray spectrum [26]. Peak separation by this software can be accomplished by running iterative calculations based on nonlinear least-squares approximations specifying the values of a series of factors, i.e., energy values and intensity ratios of each characteristic X-ray, the background shape, and estimates of the energy resolution of the detector. These include theoretical values for the energy values and intensity ratios of characteristic X-rays for each element calculated on the basis of physical phenomena. In contrast, the background shape and estimates of the energy resolution were determined experimentally on the basis of the measurement results for a sample with a simple composition, as these values are instrument-specific.

Results and discussion

Phase identification of the slip surface of the pottery

Prior to phase identification of the pigment, we tried to identify the phase of the ocherous slip lying beneath the paintings of the pottery. Figures 5 and 6 show the XRF spectrum and XRD pattern, respectively, of the slip surface of a shard of blue-painted pottery (numbered AK11-O193, belonging to the middle 18th Dynasty). To provide a wide range of information regarding the elemental composition, XRF spectra measured in white X-ray excitation mode are shown in the figures. Two sharp peaks, the K-lines of Ca and S, were observed in the ocherous slip portion of the XRF spectrum, indicating that the composition of the slip layer corresponded to that of calcareous clays containing a large amount of S. In addition, the XRD pattern (Fig. 6) confirmed that the slip layer is rich in anhydrite (CaSO_4). In addition, gypsum ($\text{CaSO}_4 \cdot 2\text{H}_2\text{O}$) and halite (NaCl) were also detected from the pattern. They would be the result of contamination during burial condition. In contrast, XRD measurements of the clay underlying the slip layer confirmed that several rock-forming minerals were present in the clay, in which there was no evidence of the presence of anhydrite. We then calculated lattice parameters of anhydrite based on the diffraction peaks, and compared these with the corresponding literature values [27]. The calculated results for an orthorhombic crystal, $a=6.975(5)$ Å, $b=6.993(3)$ Å, $c=6.236(6)$ Å, are close matches to literature values, $a=6.9933$ Å, $b=7.0017$ Å, $c=6.2411$ Å (PDF: 37-1496).

Shortland et al. have reported, on the basis of their study of museum samples of the blue-painted pottery from Malkata and Amarna, that the slip layer is rich in calcium sulfate, as confirmed by EDS (energy-dispersive spectrometry) and XRD measurement [25]. They thus focused on variations

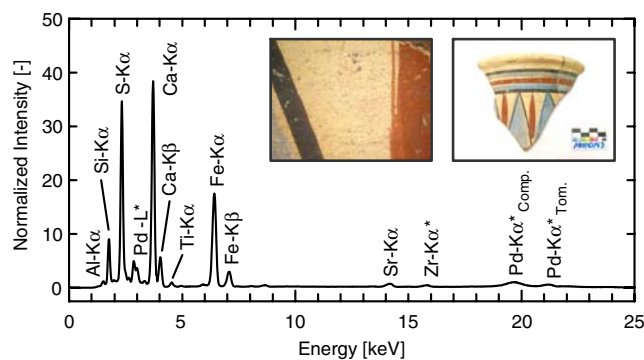


Fig. 5 X-ray fluorescence spectrum of the ocherous slip surface of blue-painted pottery

in the amount of S in the underlying clay and slip layer, and pointed out that the 2–24% SO_3 content of the slip surface shows wide variation compared with the less than 1% SO_3 content in the clay, suggesting addition of calcium sulfate to the slip. They have pointed out that this calcium sulfate in the slip layer was likely added as gypsum, which was then converted to anhydrite with the dehydration of the gypsum occurring with firing. Our results support their interpretation, which suggests that Egyptian potters used gypsum with a relatively good understanding of its function. Furthermore, Shortland et al. have suggested that gypsum observed on the surface could be the result of rehydration during burial [25]. However, we noticed that many excavated objects and stone architecture were heavily covered with salts including gypsum and halite during the burial conditions beneath the desert sands. Therefore, the latter effect is more serious, at least at our site. Peaks of Si and Fe were also detected in the XRF spectrum (Fig. 5), which are due to the clay body. This is confirmed by the fact that the diffraction peaks of rock-forming minerals, i.e., quartz (SiO_2), calcite (CaCO_3), and albite ($\text{NaAlSi}_3\text{O}_8$), were observed in the XRD pattern of the clay body (Fig. 6).

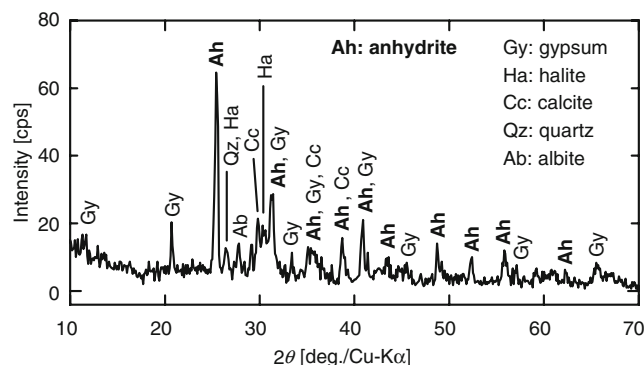


Fig. 6 X-ray powder diffraction pattern of the ocherous slip surface of blue-painted pottery

Phase identification of red pigments

XRF analysis of the red pigment on the pottery shard (AK11-O193, the middle 18th Dynasty) showed that it is rich in Fe compared with the slip surface. XRD analysis showed that hematite (Fe_2O_3), which is a typical red pigment in the New Kingdom [34], is the dominant crystalline component of the red pigment. The calculated hexagonal lattice parameters of the pigment were $a=5.037(2)$ Å, $c=13.733(13)$ Å, which are in good agreement with the literature values for hematite (PDF: 33-0664) $a=5.0356$ Å, $c=13.7489$ Å).

The red plaster pigment on the plaster (AK14-O331, the middle 18th Dynasty) was also analyzed. The XRF spectrum revealed strong Fe and Cu K lines, which are attributed to the presence of the blue plaster pigment layer underlying the red pigment layer. While there are thus a series of diffraction peaks of cuprorivaite, the result of the XRD measurement indicated that the red plaster pigment is hematite, the same as the red pigment on the blue-painted pottery.

Phase identification of black pigments

In this study, it was found, on the basis of observation by optical microscopy, that two kinds of black pigment exist in the decoration of blue-painted pottery. The major black pigment, referred to as “black pigment A” in this paper, seems to have taken on a red tinge, or it could be said that this color is brownish black. In contrast, we found some shards thickly painted with deep black pigment. This minor pigment is referred to as “black pigment B”.

A shard that was already analyzed with regard to its slip surface, blue pigment, and red pigment (AK11-O193, the middle 18th Dynasty) was decorated with black pigment A. Mn was found in the XRF spectrum of black pigment A with a significant amount of Fe. The XRD measurement indicated that the main component of this pigment is hematite, the same as the red pigment on the pottery. The calculated hexagonal lattice parameters, $a=5.038(3)$ Å, $c=13.710(21)$ Å are close to the literature values for hematite, noted previously. Thus, it is verified that the reason for the reddish tint of the black pigment A is the presence of hematite. Meanwhile, no crystalline phase containing Mn was found in the XRD pattern of the pigment.

Black pigment B painted on another shard (AK12-O172, the middle 18th Dynasty) was measured by XRF and XRD. Significant amounts of Mn and Fe were found in the XRF spectrum of the black pigment B. The XRD pattern of this pigment (Fig. 10) showed the presence of a spinel crystal, likely to be cobalt blue. Then, we examined a series of black oxide compounds containing Mn and Fe having spinel structures. Three compounds assumed as candidates

were magnetite (Fe_3O_4), jacobite (MnFe_2O_4), and Mn_3O_4 -spinel. The calculated cubic lattice parameters of black pigment B was $a=8.435(2)$ Å. This value was compared with the literature values for the three compounds under consideration, $a=8.396$ Å for magnetite (PDF: 19-0629), 8.499 Å for jacobite (PDF: 10-0319), and 8.420 Å for Mn_3O_4 -spinel (PDF: 13-0162). The result suggests that the black pigment B has a crystal structure similar to that of Mn_3O_4 -spinel. But it is very interesting that this compound has no natural occurrence as a mineral. A natural mineral with the chemical formula Mn_3O_4 , known as hausmannite, has a tetragonal crystal structure, distinct from that of the black pigment B. It is known that Mn_3O_4 -spinel is one of the products obtained by thermal transformation and can be obtained by heating manganese oxide (or carbonate, hydroxide) in air. The presence of Mn_3O_4 -spinel in the black pigment layer was also suggested by Noll et al. in their research on the pottery-paint pigments [35]. They pointed out, on the basis of their phase analysis, that formation of this phase requires a high temperature above 1000 °C. Thus, the presence of this compound will be important information for estimating the firing condition and temperature of the blue-painted pottery.

Black pigment on the plaster (AK14-O398: the middle 18th Dynasty) seems to have a brighter color than the black pigment B on the pottery. This pigment was also painted on Egyptian blue pigment, the same as the red pigment. Consequently, the measurement results contained the contaminating effect of cuprorivaite. XRF analysis of the black pigment showed that Mn and Fe exist as the major components. On the other hand, as shown in Fig. 11, XRD pattern showed the diffraction peaks of manganite ($\text{MnO}(\text{OH})$). In contrast, Sanada et al. identified pyrolusite ($\beta\text{-MnO}_2$) as the black pigment of plaster excavated from this site [9]. Lucas et al. also pointed out that pyrolusite was used as a black pigment in the New Kingdom [36]. Therefore, interesting results different from those reported previously were obtained in our work. Because both manganite and pyrolusite are widely distributed common

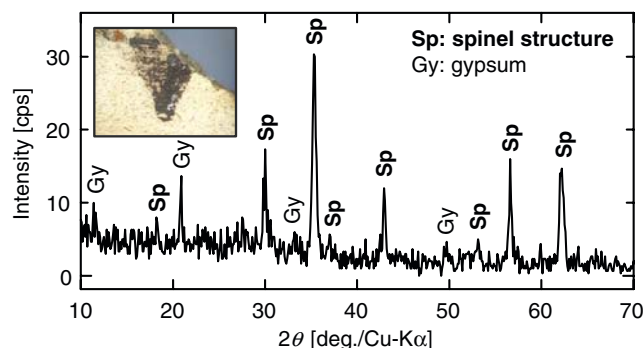


Fig. 10 X-ray powder-diffraction pattern of black pigment B on blue-painted pottery

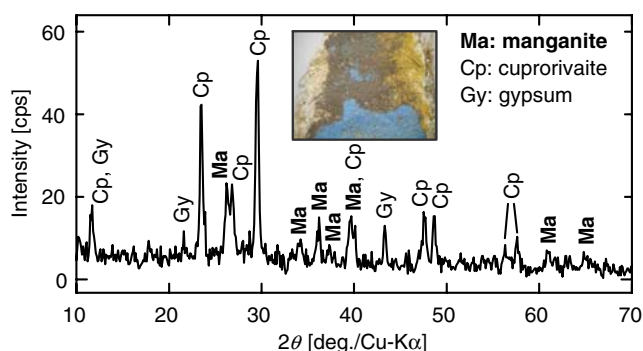


Fig. 11 X-ray powder-diffraction pattern of black plaster pigment

minerals, it cannot be denied that ancient Egyptians had mined and used both minerals. It is known that pyrolusite can be easily produced by dehydration of manganite, whereas it is difficult to obtain manganite by hydration of pyrolusite. Therefore, it is highly possible that ancient Egyptians obtained Mn in the form of manganite. Hence it is suggested that several black pigments were used in the New Kingdom, Egypt.

Compositional transition of cobalt blue

We then studied the possibility of the compositional transition of cobalt blue with time based on XRF analytical data of the blue pigment on the painted pottery. However, it is difficult to obtain accurate quantitative data for the blue pigment because the X-rays penetrate the clay body. In this study, we focused on elements unique to the blue pigment and characterized the pigment by means of a ternary diagram introducing peak-intensity ratios of these elements.

We found that the characteristic compositions of cobalt blue are Mn, Fe, Co, Ni, and Zn. But there should be questions about whether the fluorescence X-ray intensity of these elements contains contamination from the underlying layer and salts deposited on the surface. Accordingly, we examined the correlation of the peak intensity of Mn, Fe, Co, Ni, and Zn with that of other elements, as shown in Table 2, estimating the influence due to the contamination. Integrated peak intensities of these elements were obtained by peak separation using the analysis software [26] because of the peak overlap of these transition metals as described in the experimental session. A $K\alpha$ line was chosen for all of these elements because of its sharpness and high intensity. The intensity obtained was normalized by the intensity of Compton scattering peak of Pd- $K\alpha$. The peak intensity of Ca was useful for estimating the possible influence of the surface slip, the body clay, and the deposited salt. We have used the XRF spectrum with the lowest Ca intensity after analyzing several points in a shard. In addition, data for the middle 18th Dynasty were divided into two groups in this table. It was confirmed that there is no evidence of

Table 2 Correlation coefficients (r^2) of $K\alpha$ peak intensities between the elements in the cobalt blue pigment

	Middle 18th Dynasty (early half)	Middle 18th Dynasty (late half)	Later 18th Dynasty	19th Dynasty
Ca (from slip layer, body clay, and deposited salt)				
Mn	0.12	0.33	0.17	0.32
Fe	0.02	0.52	0.36	0.45
Co	0.00	0.19	0.00	0.05
Ni	0.02	0.20	0.02	0.02
Zn	0.07	0.02	0.07	0.02
Ti (from body clay)				
Mn	0.29	0.34	0.02	0.13
Fe	0.82	0.95	0.29	0.67
Co	0.24	0.18	0.00	0.01
Ni	0.17	0.25	0.00	0.03
Zn	0.05	0.01	0.04	0.01
Co (as blue colorant)				
Mn	0.52	0.70	0.51	0.40
Fe	0.30	0.29	0.23	0.03
Ni	0.78	0.85	0.88	0.97
Zn	0.70	0.74	0.85	0.65

correlation between transition metals and Ca, except for Fe. The peak intensity of Fe also shows a correlation with that of Ti, which is mostly derived from the body clay. From these results, it is found that the peak intensity of Fe is dominantly affected by the body clay underlying the pigment. On the other hand, Ni and Zn show good correlation with Co as blue colorant ($r^2=0.78$ – 0.97 and 0.65 – 0.85 , respectively), and Mn also shows moderate correlation with Co ($r^2=0.40$ – 0.70), which seems to be affected by the variation of the Mn content. In considering the use of the raw material of the cobalt blue pigment, i.e., the cobaltiferous alum, Shortland et al. compared variations of the ratio of transition metals to Co in the alum and suggested that Ni showed the highest correlation with Co, followed by Zn, whereas Mn has some variability in content [31]. Thus the observed variation of our Mn content in the pigment could be caused by that of the raw material.

We calculated two ternary diagrams to characterize the cobalt blue pigment as shown in Fig. 12(a) and (b). The peak intensity of Co, Ni, and Zn are plotted on the ternary diagram in Fig. 12(a) whereas Fig. 12(b) shows that of Mn, Ni, and Zn. It was observed that Mn, Co, Ni, and Zn levels in the blue pigment are compositionally homogeneous within a shard. This homogeneity would result from the production process: i.e., the raw material was dissolved and then the metal hydroxides were precipitated. It is found from Fig. 12 that there is a possibility of compositional transition of the cobalt blue pigment with time. The

increase in the Co ratio with time was observed in Fig. 12 (a). Besides, Fig. 12(b) seems to exhibit three compositional groups: the middle 18th Dynasty, the later 18th Dynasty, and the 19th Dynasty.

One possible explanation for these compositional transitions is a change in the composition of the raw materials, namely cobaltiferous alum. This change may be caused by a difference in the locality of the occurrence of the alum. Two places, Kharga Oasis and Dakhla Oasis, have been identified as possible sources of cobaltiferous alums [28, 32]. In addition, recent detailed study of the alum suggested that the amounts and ratios of the transition metals in the alum could vary even over a relatively small geographical area [31]. Another possibility is the change in the method of the precipitation reaction. It was reported that the variety and amount of precipitated hydroxide are affected by the concentration and variety of the alkali used in the reaction [29–31]. In fact, the hydroxides of these elements have different solubility products, so they will precipitate at different pH. The hydroxide of Al^{3+} will begin to precipitate at the lowest pH among these (pH 3.4), followed by those of Zn^{2+} (pH 6.5), Ni^{2+} and Co^{2+} (pH 7.7 and 7.8), Mn^{2+} (pH 8.6), and the hydroxide of Mg^{2+} will precipitate at the last stage (pH 9.4). Thus, it is possible to control the composition of the hydroxides of the transition metals by careful addition of alkali in the precipitation process. In addition, the color of the hydroxide precipitate is characteristic of the transition elements; visual observation could be used to control the composition of the precipitate even in ancient times.

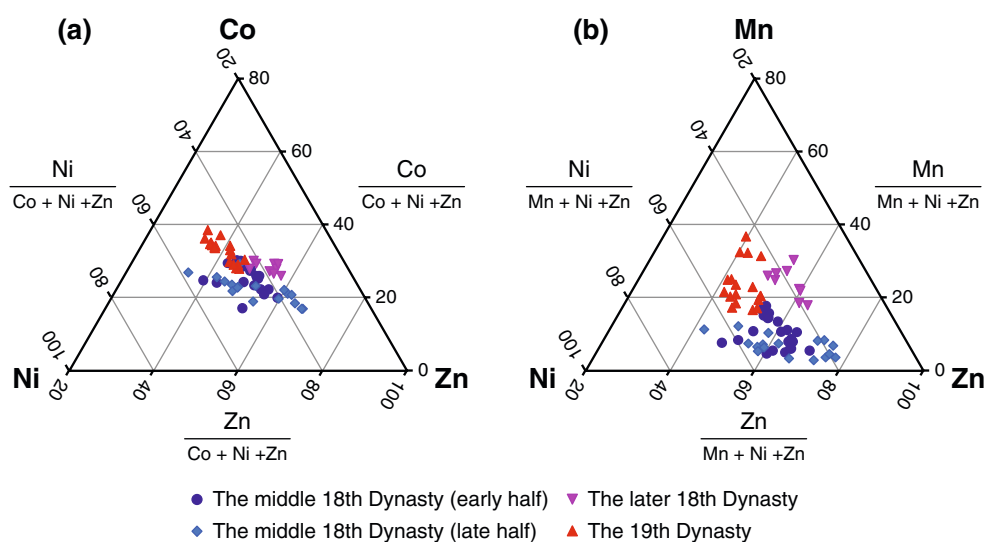
It is interesting that the ratio of Co to $\text{Co}+\text{Ni}+\text{Zn}$ seems to increase over time, as shown in Fig. 12(a). This increase in the Co content could lead to a vibrant blue color with small quantity of application. Thus this fact may provide evidence that “better quality” pigment was being produced

as the process or raw material was better understood. Large quantities of the blue pottery were used only in the New Kingdom by people in the elite class. This fact means that its production was most probably controlled by the government. In addition, a break with traditional religion, known as the “Amarna Revolution,” was carried out by Amenhotep IV in the later 18th Dynasty. Hence, it is possible to say that this religious reformation made some changes in the production of the blue-painted pottery and the cobalt blue pigment. In fact, the later 18th Dynasty was the production peak of the blue-painted pottery. It could be considered that there was a relationship between the quality modification of cobalt blue pigment and mass production of the blue-painted pottery, and this transition must most probably be the result of good understanding about raw material or production process of the cobalt blue pigment.

Conclusion

Combined use of portable XRF and XRD enable accurate phase identifications of blue, red, and black pigments of the blue-painted pottery and plaster paintings excavated from the site on the outcrop at Northwest Saqqara. Cobalt blue was identified as the blue pigment of the blue-painted pottery, whereas the other blue pigment, Egyptian blue, was used to paint plaster. Hematite was used as the red pigment for both the blue-painted pottery and plaster painting. Analysis of the black pigments suggested that several kinds of black material were used as black pigment in the New Kingdom, Egypt. Thus, much interesting information regarding the use and identification of pigments in the New Kingdom, Egypt, was obtained from our on-site analyses. Additionally, through these achievements regarding phase identification, it was demonstrated that the portable

Fig. 12 Ternary diagrams of the $K\alpha$ peak-intensity ratios of the transition metals in the cobalt blue pigment: (a) ratios for Co, Ni, and Zn; (b) ratio for Mn, Ni, and Zn (as percentages)



instruments we have developed show high levels of performance in on-site analysis. Detailed analysis of the compositional data of the blue pigment on the pottery indicated that compositional transitions of cobalt blue occurred in the New Kingdom. The transitions might be caused by changes in the procurement of raw materials or in the production process that resulted in enhanced production efficiency.

Acknowledgements The Ourstex 100FA-II portable X-ray fluorescence spectrometer was jointly developed with the Ourstex Corporation. We are deeply grateful to Mr Y. Nakajima and Mr H. Nagai. Development and improvement of a portable X-ray powder diffractometer, the X-tec PT-APXRD were jointly carried out by the Institute of X-Ray Technologies Co., Ltd. We would like to express our gratitude to Dr K. Taniguchi, Mr T. Utaka, and S. Maeo.

References

- Nakai I, Taguchi I, Yamasaki K (1991) *Anal Sci* 7 Suppl:365–368
- Dooryhée E, Martinetto P, Walter Ph, Anne M (2004) *Radiat Phys Chem* 71:863–868
- Pradell T, Molera J, Pantos E, Smith AD, Martin CM, Labrador A (2008) *Appl Phys A* 90:81–88
- Frierman JD, Bowman HR, Perlman I, York CM (1969) *Sci* 164:588
- Williams-Thorpe O, Potts PJ, Webb PC (1999) *J Archaeol Sci* 26:215–237
- Hocquet FP, Garnir HP, Marchal A, Clar M, Oger C, Strivay D (2008) *X-Ray Spectrom* 37:304–308
- Uda M, Nakamura M, Yoshimura S, Kondo J, Saito M, Shirai Y, Hasegawa S, Baba Y, Ikeda K, Ban Y, Matsuo A, Tamada M, Sunaga H, Oshio H, Yamashita D, Nakajima Y, Utaka T (2002) *Nucl Instrum Methods Phys Res Sect B* 189:382–386
- Uda M, Ishizaki A, Satoh R, Okada K, Nakajima Y, Yamashita D, Ohashi K, Sakuraba Y, Shimono A, Kojima D (2005) *Nucl Instrum Methods Phys Res Sect B* 239:77–84
- Sanada T, Hokura A, Nakai I, Maeo S, Nomura S, Taniguchi K, Utaka T, Yoshimura S (2003) *Adv X-Ray Chem Anal* 34:289–306 in Japanese
- Nakai I, Hokura A, Sanada T, Sawada T, Maeo S, Taniguchi K (2006) *Non-destr Exam Cult Objects Adv X-ray Anal* 63–69
- Nakai I, Yamada S, Hokura A, Terada Y, Shindo Y, Utaka T (2005) *X-Ray Spectrom* 34:46–51
- Kikugawa K, Abe Y, Sanada T, Nakai I (2009) *Adv X-Ray Chem Anal* 40:325–337 in Japanese
- Tantrakarn K, Kato N, Hokura A, Nakai I, Fujii Y, Gluščević S (2009) *X-Ray Spectrom* 38:121–127
- Kato N, Nakai I, Shindo Y (2009) *J Archaeol Sci* 36:1698–1707
- Maeo S, Nakai I, Nomura S, Yamao H, Taniguchi K (2003) *Adv X-Ray Chem Anal* 34:125–132 in Japanese
- Nakai I, Maeo S, Tashiro T, Tantrakarn K, Utaka T, Taniguchi K (2007) *Adv X-Ray Chem Anal* 38:371–386 in Japanese
- Abe Y, Tantrakarn K, Nakai I, Maeo S, Utaka T, Taniguchi K (2008) *Adv X-Ray Chem Anal* 39:209–222 in Japanese
- Chiari G (2008) *Nature* 453:159
- Yoshimura S, Hasegawa S (1995) *Waseda J Hum Sci* 8:177–189 in Japanese
- The Society for the Egyptian Studies of Waseda University (1995–2009) *The Journal of Egyptian Studies Occasional Publication No. 1–13*. Waseda University Press, Tokyo (in Japanese)
- Riederer J (1974) *Archaeometry* 43:483–490
- Noll W, Hangst K (1975) *Neues Jahrb Mineral Monatsh* 209–214
- Noll W (1981) In: Hughes M (ed) *Mineralogy and technology of the painted ceramics of ancient Egypt*. British Museum, London
- Hope CA (1991) *Cahiers de la Céramique Égyptienne* 2:17–92
- Shortland AJ, Hope CA, Tite MS (2006) In: Maggetti M, Messiga B (eds) *Geomaterials in cultural heritage*. Geological Society, London, pp 91–99
- IAEA (2000) WinQXAS, Quantitative X-ray Analysis System for Windows, A Software from International Atomic Energy Agency. <http://www.iaea.or.at/programmes/ripc/physics/faznic/winqxas.htm>
- ICDD (2006) *The Powder Diffraction File, PDF*. International Centre for Diffraction Data, PA
- Bachmann HG, Everts H, Hope CA (1980) *Mitt Dtsch Archäol Inst Abt Kairo* 36:33–37
- Warachim H, Rzechula J, Pielak A (1985) *Ceram Int* 11:103–106
- Rehren T (2001) *Archaeometry* 43:483–490
- Shortland AJ, Tite MS, Ewart I (2006) *Archaeometry* 48:153–168
- Kaczmarczyk A (1986) *Proc 24th Int Archaeom Symp* 369–376
- Jaksch H, Seipel W, Weiner KL, Goresy AE (1983) *Naturwissenschaften* 70:525–535
- Lee L, Quirke S (2000) In: Nicholson PT, Shaw I (eds) *Ancient Egyptian Materials and Technology*. Cambridge University Press, Cambridge, pp 104–120
- Noll W, Holm R, Born L (1975) *Angew Chem Int Ed* 14:602–613
- Lucas A, Harris JR (1962) *Ancient Egyptian Material and Industries*, 4th edn. Hodder and Stoughton Educational, London